Journal of
Chemical Engineering & Process Technology

Farzi et al., J Chem Eng Process Technol 2014, 5:5
DOI: 10.4172/2157-7048.1000201

Research Article Open Access

Droplet Size Distribution in a Kenics Static Mixer: CFD Simulation and Experimental Investigation of Emulsions

Farzi GA[1]*, Reza-Zadeh N[2] and Parsian Nejad A[2]

[1]Material and Polymer Engineering Department, Hakim Sabzevari University, Sabzevar, Iran
[2]Mechanical Engineering Department, Hakim Sabzevari University, Sabzevar, Iran

Abstract

The minimum achievable droplet sizes created by a simple in-line Kenics Static Mixer (KSM) under various flow rates and mixing time in oil in water (O/W) emulsion were investigated through turbulent flow system. First, a Computational Fluid Dynamics (CFD) method is utilized to predict final droplet sizes in different Reynolds number. Then, an experimental setup was used in order to validate CFD results. The droplet size was monitored using Dynamic Light Scattering (DLS) technique by means of a Malvern zetasizer machine. Breakup/coalescence of droplets under constant volume fractions of oil was studied when flow rate was varied from 36.7 to 85 ml/s. Results showed that droplet size distribution highly depends on flow rate and mixing time. Droplets break more easily and faster at higher flow rates. The results proved that the obtaining small enough droplets using static mixer in less than 40 minutes at the flow rates above 36.7 ml/s at moderate concentration of oil volume fraction.

Keywords: Two phase flow; Emulsion; Droplet sizes; Kenics Static Mixer; CFD

Introduction

Over recent years a great deal of attention has been paid to the formation and stability of micro/nano scale emulsions and precise control of droplet size and size distribution [1]. Two phase liquid dispersion is one of the most complex processes among mixing operations. Agitating two immiscible liquids results in the dispersion of one phase in the other in the form of small droplets whose characteristics depend on the equipment and the operating conditions [2]. It is practically impossible to make stable dispersions of uniform droplet size distribution, because of the wide range of properties and flow conditions [3]. A large amount of work can be found in the literature concerning the prediction of drop size distributions in turbulent liquid-liquid dispersions in static mixers (SM). Most of them use the concept of a turbulent energy cascade to predict the maximum stable droplet diameter, referring to the Hinze-Kolmogorov theory [2-8].

Static mixers are introduced as an alternative device believed to have a significant industrial potential to produce stable emulsions [9]. While SMs are widely used in other agro and petrochemical processes, they have not been studied in depth for the generation of mini-emulsion droplets. It is clear that they can be economically practical, safely used and can be utilized on larger scales. However, in terms of dispersion systems, their role in droplet breakage is an area of ongoing research. In our previous work [10], we reported a successful experimental production of mini-emulsions which was produced by making the mixture circulate two immiscible liquids (oil and aqueous phases) through the pipe in which the SM was inserted.

In this investigation, a CFD code is used to calculate the flow in the KSM and results are validated by means of DLS measurements of a final droplets diameter in a specific time. In the first section, the numerical methods and governing equations are proposed and the model and simulation properties are described. In the second section, two cases in the same manner of experimental setup but different in order of flow rate are defined and material properties are described. Finally, the CFD results are compared with the experimental results to evaluate the results, then numerical results and the dynamic behavior of the KSM is discussed in more detail.

Theoretical Model-Numerical Methodology

Breakup of bubbles and droplets, has been the subject of investigation for several decades starting with the pioneering work by two researchers, Kolmogorov [11] and Hinze [12], who proposed a formula for the maximum drop size, independently. Thereafter, Luo base on spherical assumption of droplet shapes proposed a model for breakup of fluid drop, description of the stability of mono-dispersed colloids, Population Balance Equations (PBEs) have found diverse applications in areas involving particulate systems [13]. Recently, Solsvik proposed an algebra of the high-order least-squares method, which linked to the implementation issues of a problem describing the drop size distribution within a liquid-liquid emulsion [14]. The high-accuracy, low numerical diffusion of the least-squares method for these types of solution has been proved, regarding the published literatures [15-18].

In this work, a 3D CFD model of the two-phase flow in continuous KSM is developed. Based on an Eulerian-Eulerian two-fluid model, the high-order least-squares method (HOLS) is used to solve the PBE [19]. The PBE and CFD models are both solved by the non-commercial CFD code developed by our researcher team.

A general form of the population balance equation can be expressed as follows:

$$\frac{\partial_n(L;x,t)}{\partial_t}+\nabla.[\vec{u}n(L;x,t)]=-\frac{\partial}{\partial L}[G(L)n(L;x,t)]+B_{ag}(L;x,t)-D_{ag}(L;x,t)+B_{br}(L;x,t)-D_{br}(L;x,t) \quad (1)$$

Where, $n(L;x,t)$ is the number density function with droplet diameter (L) as the internal coordinate, G(L)$n(L;x,t)$ is the droplet flux due to molecular growth rate, $B_{ag}(L;x,t)$ and $D_{ag}(L;x,t)$ are the birth and

***Corresponding author:** Farzi GA, Material and Polymer Engineering Department, Hakim Sabzevari University, Sabzevar, Iran, Tel: 989373537388; E-mail: alifarzi@yahoo.com

Received June 02, 2014; **Accepted** July 22, 2014; **Published** July 25, 2014

Citation: Farzi GA, Reza-Zadeh N, Parsian Nejad A (2014) Droplet Size Distribution in a Kenics Static Mixer: CFD Simulation and Experimental Investigation of Emulsions. J Chem Eng Process Technol 5: 201. doi: 10.4172/2157-7048.1000201

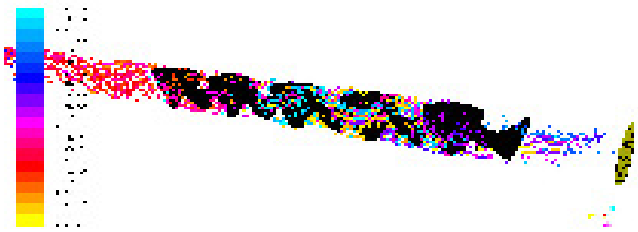

Figure 1: Illustration of the SM using CFD model.

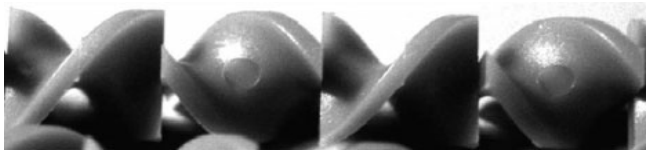

Figure 2: Physical shape of Kenics static mixer.

name	First Case		Second Case	
	material	amount	material	amount
Continues phase	de-ionized water	60% (211 g)	de-ionized water	85% (418 g)
Dispersed phase	methyl methacrylate (MMA)	40% (84.4 g)	sunflower oil	15% (72 g)
surfactant	sodium dodecyl sulfate (SDS)	1 g/L	sodium dodecyl sulfate (SDS)	0.4 g/L

Table 1: Emulsion Recipes.

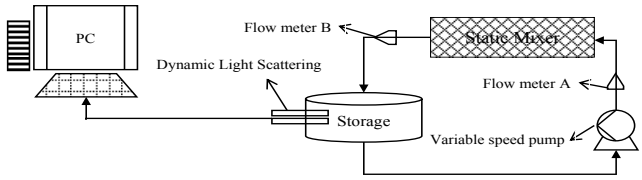

Figure 3: Schematic diagram of the experimental setup.

death rate of droplets diameter (L) due to aggregation, respectively, and $B_{br}(L;x,t)$ and $D_{br}(L;x,t)$ are the birth and death rate of droplets diameter (L) due to breakage, respectively. In eqn 1, the first term on the left hand is the transient term, the second term is the convective term, and the terms on the right hand are the source term describing droplet growth, aggregation, and breakage dynamics, respectively.

Regarding to its actual properties, the simulated SM has an inner diameter of 25 mm, a height of 25 mm, and 10 standard static elements fabricated from polyacetal plastic, arranged alternatively at 90° (Figure 2). In addition, Grid sensitivity was carried out initially, and the results indicated that a total amount of 325 K cells was adequate to conserve the mass of each phase in the dynamics model.

In order to obtain suitable mesh size in our CFD model at initial step, fluid velocity was varied from 0.11 to 10 m/s which provides Reynolds number from 3 K to 280 K and mesh size was adapted for minimal error based on numerical and experimental Re number. Significant differences was seen for course mesh size, however, after re-meshed the model with super fine mesh, ($\sim 10^{-6}$) when looking at the overall flow characteristics, which are shown below, one can see that the differences are not too large and in general they agree well. Detailed information of mesh independency study and prediction errors is presented in Table 2.

It should be note that, although the physical geometries of SM is adapted with model (Figure 1), there may exist some differences between results of our model and experiments due to small deviation of SM geometry and other assumptions.

The phase-coupled SIMPLE (Semi-Implicit Method for Pressure Linked Equations) algorithm was used to couple pressure and velocity [20]. A one stage calculation and two cases with different Reynolds numbers were implemented. The flow field was simulated with bulk velocity started from 36.7 ml/s, 60.6 ml/s and 62 ml/s in the first case and 36.7 ml/s up to 82 ml/s in the second case. Then results were compared with those obtained experimentally from DLS technique. The breakage and coalescence process was simulated by utilizing the energy and PBE model regarding droplet tracing technique until the average nano-size Sauter mean diameter (d_{32}) reached. It should be noted that since sufficient amount of literatures proved there is negligible ratio of breakage occurs in storage tank compared to those in SM, droplet breakage in storage can be disregarded [9,10,21-23].

Experimental

To carry out the experimental studies two cases were considered for oil phases; methyl methacrylate (MMA) and sunflower oil. In both systems de-ionized water was used as continuous phase. General formulations of mini-emulsions are shown in Table 1.

In the second case, Sunflower oil as dispersed has a density of 902.4 kg/m^3, Refractive index of 1.4646, and viscosity of 47.11 g/m.s, all measured at 25°C.Geometry and dimensions of SM were modeled using Solid Works 3D CAD software, and exported into commercial software GAMBIT 2.1 and an appropriate mesh is generated.

A schematic diagram of the experimental setup is provided in Figure 3. A circulator pump was made to function with variable electrical current to ensure a series of known flow-rates. The mixture of two immiscible fluids was pumped from a 2 liter capacity reservoir to the SM. The fluid flow unit consists of piping section (with inner diameter of 25 mm and total piping lengths of 1571 mm) preceded by an inlet section where two phases are co-axially introduced into the piping section without any pre-mixing process. However, immediately after entrance into the pipe they mixed due to the turbulence fluid flow system. As mentioned previously, the oil droplet size was measured by DLS after certain time achieving steady state condition. Furthermore, a feedback system is used to measure the flow rate.

Results and Discussion

At the initial phase of the validation process, the results of experimental emulsification using the KSMs according to first formulation were compared with those obtained from CFD model. These experimental results were previously published elsewhere [10]. Figure 4 shows droplet size as emulsification time. In this figure the points to the graph are experimentally captured for different flow rates, whereas the lines indicate calculated values using CFD code.

Regarding to the Figure 4, droplet diameter decreasing asymptotically with increasing homogenization time and smaller droplet obtained at higher flow rates. In other respects, an increase in mechanical energy can help overcome the limit imposed by interfacial tension, thereby inducing more breakage. One might theorize that at higher flow rates, more energy is input into the system allowing breaking up large droplets. By means of that, intensifies the distribution

Re. No.	100		200		400		800		1.2 k		12 k		50 k		80 k		120 k	
Mesh Size	Pre. Err. %	Vel. Pro. Err. %	Pre. Err. %	Vel. Pro. Err. %	Pre. Err. %	Vel. Pro. Err. %	Pre. Err. %	Vel. Pro. Err. %	Pre. Err. %	Vel. Pro. Err. %	Pre. Err. %	Vel. Pro. Err. %	Pre. Err. %	Vel. Pro. Err. %	Pre. Err. %	Vel. Pro. Err. %	Pre. Err. %	Vel. Pro. Err. %
10^{-1}	725	911	608	552	-	-	-	-	-	-	-	-	-	-	-	-	1332	1592
10^{-2}	408	391	418	382	427	371	-	-	-	-	-	-	-	-	-	-	528	717
10^{-3}	244	212	238	203	217	193	225	201	-	-	-	-	-	-	-	-	-	-
10^{-4}	68	118	72	128	59	113	73	141	68	140	-	-	-	-	-	-	-	-
10^{-5}	16	33	19	25	12	16	14	22	11	16	9	13	13	15	17	26	14	18
10^{-6}	16	31	17	21	13	15	14	21	10	14	9	14	12	15	14	23	16	21
10^{-7}	17	38	17	20	11	10	12	20	7	11	10	12	12	14	14	23	14	20

Table 2: Mesh Independency Results. Pre. Err=Prediction Error, Vel. Pro. Err=Velocity Profile Error.

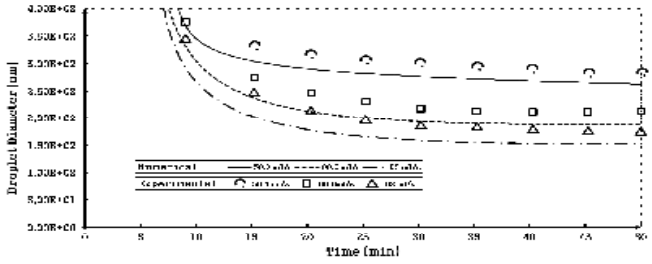

Figure 4: First case - Computational and experimental evolution of the droplets size (d_s) over mixing time.

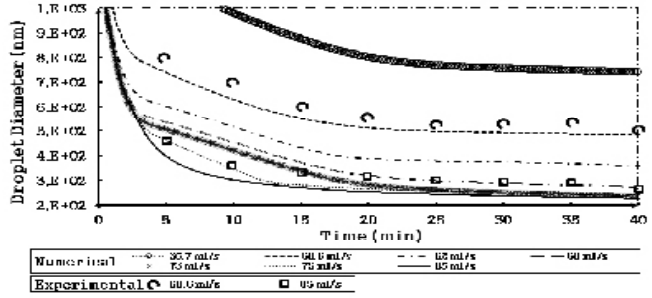

Figure 5: Second case - Computational and experimental evolution of the droplets size (d_s) over mixing time.

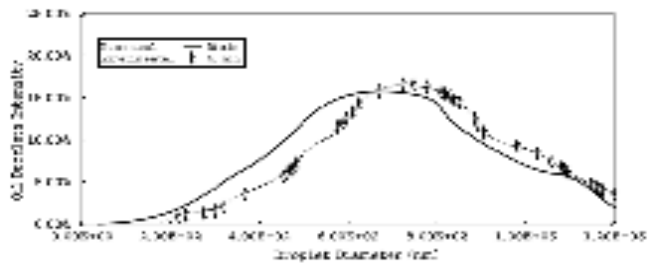

Figure 6: Second case –Numerical and experimental oil droplet size distributions at 40 minutes for the 36.7 ml/s flow rate.

and decreases the average size. This leads to narrow distribution droplet size.

Considering Figure 4, discrepancy between the CFD and experimental results for 36.7 ml/s flow rates in 6 times interval are, 28, 31, 27, 35, 32 and 29 nm respectively, with total computational discrepancy about 14%. These results have been 35, 27, 41, 36, 32 and 27 with total computational discrepancy about 18% for 60.6 ml/s flow rate. Similarly, the results shows about 45, 42, 37, 31, 29 and 30 nm mismatch in droplet size at 62 ml/s flow rate and 21% of total computational discrepancy.

Figure 5 shows the effect of different flow rates on the mean droplet size at fixed values of the sunflower oil and surfactant concentrations. The flow rate was set to 60.6 and 85 ml/s for experiments and varied from 36.7 to 85 ml/s for numerical studies. As it can be seen, at 60.6 ml/s flow rate, the experimental data shows larger droplets than numerical results. When flow rate is higher than 68 ml/s from the beginning of process for few minutes droplet diameter of emulsion is in good accordance with those of CFD results. However, in general there is a meaningful difference between experimental and CFD results. This is due to the fact of the problem of "lost" droplets, saying, droplet trajectories are trapped near a solid wall accentuate in lower flow rates [21].

The experimental results of 85 ml/s flow rates shows relatively lower difference of droplet size between numerical and experimental results in compared with those obtained for lower flow rates.

With increasing flow rate, the Non-linear relationship between the flow rate and the average droplets size appears even at first stage of emulsification.

In order to evaluate the validity of our CFD model results for a given homogenization time, droplets size of emulsion prepared within 40 minutes at 36.7 ml/s flow rate is compared with those obtained from numerical data in Figure 6. This figure clearly displays similar trends for numerical and experimental results.

It is possible to determine the frequency of coalescence and breakup for numerical results in Figure 6. This may help us to have an idea for experimentally coalescence and breakup of droplets. The brakeage of droplet has been studied extensively, the incorporation of two different breakage behavior that accounted for large droplets to break easier due to turbulent shear [24,25] and on the other hand, small droplets break due to collisions between droplets and turbulent eddies [26,27].

However, theoretical and experimental results are not ideally matched, but in order to gain an insight to the results of previous investigations it is worthy to discuss the frequency of coalescence and break up of droplets based on Figure 6 in three different group of smaller than 400 nm, between 400-800 nm and larger than 800 nm. Where,

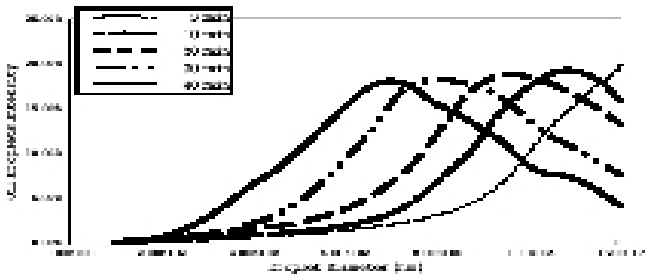

Figure 7: Second case - Oil droplet size distributions at 5, 10, 20, 30 and 40 minutes for the 36.7 ml/s flow rate

Flow rate (ml/s)	Homogenization time (min)	Average Num. Err. (%)		
		Under 400 nm	400 to 800 nm	Over 800 nm
36.7	*5*	12.51	*19.28*	*13.25*
	10	18.92	*17.05*	*12.08*
	20	18.26	*21.59*	*23.24*
	30	13.85	*16.12*	*21.25*
	40	20.82	*23.20*	*28.56*
60.6	*5*	14.28	21.02	14.70
	10	13.25	19.66	14.86
	20	16.02	23.74	24.00
	30	15.11	16.83	21.63
	40	16.28	17.47	17.68
62	*5*	13.80	15.84	19.83
	10	12.52	15.36	16.80
	20	25.53	17.70	19.18
	30	19.28	18.63	18.92
	40	17.28	18.95	24.84
68	*5*	14.50	17.67	15.19
	10	17.08	16.92	18.22
	20	24.53	17.51	17.16
	30	16.24	22.93	22.16
	40	15.23	23.56	13.12
73	*5*	17.52	14.14	16.90
	10	23.89	16.47	19.29
	20	24.57	23.72	17.54
	30	21.99	15.08	21.67
	40	16.29	16.48	24.06
75	*5*	17.24	16.93	16.02
	10	19.82	22.62	17.70
	20	23.87	19.79	15.93
	30	16.55	13.47	22.03
	40	13.83	13.60	22.86
85	*5*	17.91	15.53	*17.81*
	10	22.88	12.51	*19.11*
	20	18.01	15.39	*21.40*
	30	18.63	21.90	*18.21*
	40	24.21	15.77	*15.09*

Table 3: Discrepancies in the computational and experimental results.

numerical results for the average frequency of droplets under 400 nm showed average coalescence of $1.243\times E10^{6}$ and $8.315\times E10^{2}$ of breakage per droplet. Whereas, these values are $6.218\times E10^{4}$ and $2.386\times E10^{4}$ for second group and also $9.624\times E10^{2}$, $9.582\times E10^{8}$ for third group, respectively. These results only calculated during the time a droplet was a member of the groups. These comparison shows that smaller droplets tend to more coalescence and larger droplets should break up more frequently than smaller ones. These results are in agreement with those of other researchers. If the previously described breakage frequency is valid, then our experimental data supports the dependency of the breakage efficiency to the droplet size. Regarding the numerical data there is negligible breakage rates predicted for small droplet sizes.

It is reported that the coalescence of droplets, depends on the evolution of overall surface area and shape of drops [28,29] and/or on the diameter of drops [30] and/or on the volume of the droplet [30,31]. Now it is interesting to turn our attention to check whether or not these well-founded phenomena may satisfy with our CFD results. Since we use PBEs, the exact number of droplets is available for each of previously mentioned groups of droplets. It was determined that the number of droplets under 400 nm is only 2.89% of total number of droplets, while those between 400 to 800 nm are 39.24% and larger than 800 nm are 57.87%. Based on these results total surface area of droplets are $5.292\times E10^{9}$ nm^2, $2.634\times E10^{14}$ nm^2 and $1.109\times E10^{14}$ nm^2 for droplets groups less than 400 nm, between 400-800 nm and larger than 800 nm, respectively.

Thus, considering the total surface area of droplets in compare with coalescence and breakage rate reveals a logical conformity with respect to previews judgment; this means that the coalescence rate strongly depends indirectly on the droplet size and with decreasing droplet sizes, harmonically increasing total droplets surface area, coalescence frequency increased in agreement.

Figure 7 shows numerical results of oil droplet size distributions after 5, 10, 20, 30 and 40 minutes of homogenization for the 36.7 ml/s flow rate. One can see as the slope of the 5 min indicator curve increased dramatically after 900 nm droplet size, the ratio is express limitation of droplet breakage to the 900 nm.

It also reproduced the positive trend that the mean diameter decreased with increasing homogenization time. However, the numerical results show some difference in droplet diameter, especially for the lowest flow rates. Taken collectively, these results suggested that the functional dependencies of the mixing time and breakage rate was reasonable but that quantitative predictions with the base case model parameters may be difficult. Below also provided further numerical details of the full drop size distribution (See Table 3).

Conclusions

Droplet breakage using KSM has been simulated by means of CFD technique. In the preliminary validation stage, the simulation has captured the droplet changes successfully and reasonable difference between computed and measured results was shown. Fluid flow rate, mean droplet size and homogenization time were considered as important parameters. The CFD results were evaluated for two experimental systems with different oil phase. Droplet size was measured for these systems using Dynamic Light Scattering method. In theoretical model mesh size was adapted for our system using mesh dependency studies. Comparing theoretical results and experimental results may pursuit one that population balance equations can be suitable technique to simulate droplet creation at homogenization process. A more in depth study considering much more parameters is required to gain better understanding of homogenization process using SM.

References

1. Chang-Hyung C, Weitz DA, Lee CS (2013) One step formation of controllable complex emulsions: from functional particles to simultaneous encapsulation of hydrophilic and hydrophobic agents into desired position. Advanced Materials 25: 2536-2541.

2. Musa SH, Basri M, Masoumi HRF, Karjiban RA, Malek EA, et al. (2013) Formulation Optimization of Palm Kernel Oil Esters Nano emulsion-Loaded with Chloramphenicol suitable for Meningitis Treatment. Colloids and Surfaces B: Biointerfaces 112: 113-119.

3. MeeRyung L,Ha-Neul C, Ho-Kyung H, Won-Jae L (2013) ARTICLE: Production and Characterization of Beta-lactoglobulin/Alginate Nanoemulsion Containing Coenzyme Q_10: Impact of Heat Treatment and Alginate Concentrate. Korea food science of animal resources 33: 67-74.

4. Sheeran PS, Matsunaga TO, Dayton PA (2013) Phase-transition thresholds and vaporization phenomena for ultrasound phase-change nanoemulsions assessed via high-speed optical microscopy. Physics in medicine and biology 58: 4513.

5. Sanela DM, Nebojsa CD, Tanja IM, Jela RM, Milic, Gordana VM, et al. (2013) Nanoemulsions produced with varied type of emulsifier and oil content: An influence of formulation and process parameters on the characteristics and physical stability. Hemijskaindustrija 67: 795-809.

6. Schmidt J, Damm C, Romeis S, Peukert W (2013) Formation of nanoemulsions in stirred media mills. Chemical Engineering Science 102: 300-308.

7. Mat Hadzir N, Basri M, Abdul Rahman MB, Salleh AB, Raja Abdul Rahman RN, et al. (2013) Phase behaviour and formation of fatty acid esters nanoemulsions containing piroxicam. AAPS PharmSciTech 14: 456-463.

8. Campardelli R, Cherain M, Perfetti C, Iorio C, Scognamiglio M, et al. (2013) Lipid Nanoparticles production by supercritical fluid assisted emulsion-diffusion. The Journal of Supercritical Fluids 82: 34-40.

9. El-Jaby U, Farzi G, Lami EB, Cunningham M, Timothy MF (2009) Emulsification for latex production using static mixers. In Macromolecular Symposia 281: 77-84.

10. Farzi G, Mortezaei M, Badiei A (2011) Relationship between droplet size and fluid flow characteristics in miniemulsion polymerization of methyl methacrylate. Journal of Applied Polymer Science 120: 1591-1596.

11. Tikhomirov VM (1991) On the breakage of drops in a turbulent flow. Selected Works of A. N. Kolmogorov Mathematics and Its Applications (Soviet Series) Volume 25: 339-343.

12. Hinze JO (1955) Fundamentals of the hydrodynamic mechanism of splitting in dispersion processes. AIChE J 1: 289-295.

13. Luo H, Svendsen HF (1996) Theoretical model for drop and bubble breakup in turbulent dispersions. AIChE J 42: 1225-1233.

14. Solsvik J, Jakobsen HA (2014) Solution of the dynamic population balance equation describing breakage–coalescence systems in agitated vessels: The least squares method. The Canadian Journal of Chemical Engineering 92: 266-287.

15. Solsvik J, Jakobsen HA (2013) On the solution of the population balance equation for bubbly flows using the high-order least squares method: implementation issues. Reviews in Chemical Engineering 29: 63-98.

16. Solsvik J, Borka Z, Becker PJ, Sheibat-Othman N, Jakobsen HA (2014) Evaluation of breakage kernels for liquid–liquid systems: Solution of the population balance equation by the least-squares method. The Canadian Journal of Chemical Engineering 92: 234-249.

17. Bork Z, Jakobsen HA (2012) Evaluation of breakage and coalescence kernels for vertical bubbly flows using a combined multifluid-population balance model solved by least squares method. Procedia Engineering 42: 623-633.

18. Solsvik J, Jakobsen HA (2013) Evaluation of weighted residual methods for the solution of a population balance model describing bubbly flows: The least-squares, galerkin, tau, and orthogonal collocation methods. Industrial & Engineering Chemistry Research 52: 15988-16013.

19. Santos FP, Favero JL, Lage PLC (2013) Solution of the population balance equation by the direct dual quadrature method of generalized moments. Chemical Engineering Science 101: 663-673.

20. Reddy NS, Rajagopal K, Veena PH, Pravin VK (2013) A Pressure Based Solver for an Incompressible Laminar Newtonian Fluids. International Journal of Fluids Engineering 5: 21-28.

21. Talansier E, Dellavalle D, Loisel C, Desrumaux A, Legrand J (2013) Elaboration of controlled structure foams with the SMX static mixer. AIChE Journal 59: 132-145.

22. Baumann A, Jeelani SAK, Holenstein B, Stössel P, Windhab EJ (2012) Flow regimes and drop break-up in SMX and packed bed static mixers. Chemical Engineering Science 73: 354-365.

23. Meijer HEH, Singh MK, Anderson PD (2012) On the performance of static mixers: A quantitative comparison. Progress in Polymer Science 37: 1333-1349.

24. Rafiee M, Simmons MJH, Ingram A, Stitt EH (2013) Development of positron emission particle tracking for studying laminar mixing in Kenics static mixer. Chemical Engineering Research and Design 91: 2106-2113.

25. Lee L, Hancocks R, Noble I, Norton IT (2014) Production of water-in-oil nanoemulsions using high pressure homogenisation: A study on droplet break-up. Journal of Food Engineering 131: 33-37.

26. Focke C, Kuschel M, Sommerfeld M, Bothe D (2013) Collision between high and low viscosity droplets: Direct Numerical Simulations and experiments. International Journal of Multiphase Flow 56: 81-92.

27. Kunnen RPJ, Siewert C, Meinke M, Schröder W, Beheng KD (2013) Numerically determined geometric collision kernels in spatially evolving isotropic turbulence relevant for droplets in clouds. Atmospheric Research 127: 8-21.

28. Munz M, Mills T (2014) Size dependence of shape and stiffness of single sessile oil nanodroplets as measured by atomic force microscopy. Langmuir 30: 4243-4252.

29. Ata S, Pugh RJ, Jameson GJ (2011) The influence of interfacial ageing and temperature on the coalescence of oil droplets in water. Colloids and Surfaces A: Physicochemical and Engineering Aspects 374: 96-101.

30. Mertaniemi H, Forchheimer R, Ikkala O, Ras RH (2012) Rebounding droplet-droplet collisions on superhydrophobic surfaces: from the phenomenon to droplet logic. Adv Mater 24: 5738-5743.

31. Heng F, Striolo A (2012) Mechanistic study of droplets coalescence in Pickering emulsions. Soft Matter 8: 9533-9538.